Photoinduced Electron Transfer from 3-(9-Anthracene)propyltrimethyl Ammonium Bromide and Pyrene to Methyl viologen on the Surface of Polystyrene Latex Particles

Yong-Kuan Gong, Tsuyoshi Miyamoto, and Kenichi Nakashima*

Department of Chemistry, Faculty of Science and Engineering, Saga University, 1 Honjo-machi, Saga 840-8502, Japan

Shuichi Hashimoto

Department of Chemistry, Gunma College of Technology, 580 Toriba-machi, Maebashi, Gunma 371-0845, Japan

Received: November 4, 1999; In Final Form: March 20, 2000

Photoinduced electron transfer from anthracene (An), 3-(9-anthracene)propyltrimethylammonium bromide (APTAB), and pyrene (Py) to methyl viologen (MV^{2+}) in polystyrene (PS) latex dispersions has been studied by steady-state fluorescence, time-resolved fluorescence, and diffuse reflectance flash photolysis spectroscopy. Steady-state fluorescence measurements showed that the photoinduced electron transfer from APTAB and Py to MV^{2+} is remarkably enhanced on going from the aqueous homogeneous solution to the latex dispersion, whereas no such significant latex effect is observed for the An−MV^{2+} pair. This seems to be because An molecules deeply penetrate into the latex particles in contrast to APTAB, Py, and MV^{2+}. The fluorescence decay curves of APTAB in PS latex dispersions are conformed to double-exponential functions. The analysis reveals that quenching of APTAB fluorescence by MV^{2+} (i.e., photoinduced electron transfer from the former to the latter) on PS latex surfaces is performed by both static and dynamic mechanisms. The diffuse reflectance laser flash photolysis study revealed that back electron transfer from the $MV^{\bullet+}$ cation radical to the $Py^{\bullet+}$ cation radical is markedly suppressed in the PS latex dispersion.

1. Introduction

Latex particles represent a new type of organic solid material that can be used as a microsubstrate for photoreactions. The surface consists of organic polymers embedded sparsely with functional groups such as sulfate, carboxyl, or amino groups. This structure leads latex particles to have two kinds of adsorption sites on the surface: (1) the polymer matrix, which affords continuous adsorption domains to nonpolar and less polar adsorbates, and (2) the functional group, which gives discrete adsorption sites to ionic and highly polar species. Such a feature has not been seen in any other solid materials. Furthermore, latex particles have many other features as follows: (1) various kinds of functional groups can be introduced onto the latex surfaces; (2) the concentration of the functional groups on latex surfaces can be controlled easily by modern synthesis techniques; (3) different types of polymers such as polystyrene (PS) and polyacrylates, with varying degrees of polarity, can be used as the support material; (4) the particle shape is highly uniform (spherical); (5) the particle size can be controlled within a narrow distribution.

We have investigated several photoreactions on the surface of PS and poly(butyl methacrylate) latexes in aqueous dispersions. The photoreactions so far investigated include electronic energy transfer from rhodamine dyes to malachite green,[1,2] photoinduced electron transfer (PET) from 1-pyrenemethanol and pyrene to methyl viologen,[3,4] PET from indolic compounds to 1-pyrenemethanol,[5] and excimer formation of pyrene derivatives.[6] On going from a homogeneous aqueous solution to the latex dispersion, the efficiencies of the photoreactions are enhanced dramatically. In this article, we report studies of PET from anthracene (An), its derivative, and pyrene (Py) to methyl viologen (MV^{2+}) on the surface of PS latex particles in aqueous dispersions. The An derivative used is 3-(9-anthracene)propyl trimethylammonium bromide (APTAB), which is expected to be effectively adsorbed onto the latex surface because of the electrostatic interaction between the trimethylammonuim group of APTAB and the sulfate group on the latex surface.

The fluorescence of the donors (Ds) used is quenched by MV^{2+} through PET as follows[7−11]:

SCHEME 1

$$D + h\nu_a \xrightarrow{Abs.} D^*$$

$$D^* + MV^{2+} \xrightarrow{PET} D^{\bullet+} + MV^{\bullet+}$$

$$D^* \downarrow Fluorescence \quad D + h\nu_f$$

According to this scheme, we observed the PET reaction by monitoring the fluorescence quenching of APTAB, An, and Py. Steady-state fluorescence measurements, show that the PET from APTAB and Py to MV^{2+} is remarkably enhanced on going from the aqueous homogeneous solution to the latex dispersion, whereas no such marked latex effect is observed for the An−MV^{2+} pair. This difference is discussed on the basis of the adsorption isotherms of the donors and acceptor onto the latex particles. Time-resolved fluorescence studies revealed that PET

* Corresponding author: Department of Chemistry, Faculty of Science and Engineering, Saga University, 1 Honjo-machi, Saga 840-8502, Japan E-mail: nakashik@cc.saga-u.ac.jp

10.1021/jp993898r CCC: $19.00
Published on Web 05/24/2000

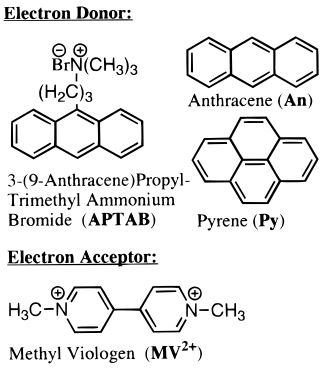

Figure 1. Structural formulas of electron donors and an acceptor.

from APTAB to MV^{2+} on PS latex surfaces is operated by both static and dynamic mechanisms.[12,13] Diffuse reflectance laser flash photolysis study revealed that back electron transfer from $MV^{\bullet+}$ cation radical to $Py^{\bullet+}$ cation radical is markedly suppressed on the PS latex particles.

2. Experimental Section

APTAB (Molecular Probes, Inc.) and An (Tokyo Kasei Kogyo Co., Ltd.; zone-refined sample) were used as received. MV^{2+} from Katayama Chemical Co. Ltd., was guaranteed grade and used without further purification. Py was purified by vacuum sublimation. Structural formulas of these compounds are shown in Figure 1. Water was purified with a Millipore Milli Q purification system.

Styrene monomer was washed first with 2% sodium hydroxide solution, then with Milli Q water, followed by vacuum distillation. Two anionic PS latexes, LS12 and LS15, which contained negatively charged surface sulfate groups, were studied. LS12 was synthesized by standard emulsion polymerization in the presence of sodium dodecyl sulfate[1] and LS15 was synthesized according to the recipe of the latex CG5 used by Charreyre et al.[14] The latexes were dialyzed repeatedly against water until the conductivity of the serum was reduced to that of Milli Q water. Diameters of the latex particles were determined with an Otsuka ELS-800 dynamic light-scattering spectrophotometer. The mean diameter of LS12 is 182 nm and of LS15, 85 nm; both LS12 and LS15 have a narrow size distribution.

Stock solutions of APTAB and MV^{2+} in water were prepared to give concentrations 50 μM and 20 mM, respectively. Py and An have very low solubility in water (0.6 and 0.3 μM, respectively).[15,16] Therefore, the methanol solutions of An and Py were used as the stock solutions, and the solvent was completely removed by N_2 purging before mixing with the PS particles. Portions of the PS dispersion and donor/acceptor stocks were mixed in a 10-mL volumetric flask, followed by sonication for 5 min. The samples were stored in the dark for 1 day before the spectroscopic measurements. In fluorescence experiments, the samples were deaerated by N_2 purging for 15 min unless otherwise mentioned.

Adsorption isotherms of APTAB, An, Py, and MV^{2+} onto the latex surfaces were measured by ultracentrifugation. Portions of the latex dispersion containing known amounts of the probe were centrifuged with Beckman Avanti-30 ultracentrifuge for 60 min at 2.60×10^4 rpm ($5.70 \times 10^4 g$) for LS12 or an Hitachi 55P-72 ultracentrifuge for 30 min at 4.00×10^4 rpm ($1.05 \times 10^5 g$) for LS15. Concentration of the probe in the supernatant after centrifugation was determined by fluorescence spectroscopy. No detectable self-quenching effect occurs in APTAB, though the concentration is high. The amount of the probe adsorbed was calculated from the difference of the total concentration in the dispersion and equilibrium concentration in the serum.

Fluorescence spectra were recorded on a Hitachi F-4000 spectrofluorometer. The spectra were corrected by use of a standard tungsten lamp with a known color temperature. Steady-state fluorescence intensity is expressed in terms of peak height of a maximum band, unless otherwise stated. Absorption spectra were measured with a Jasco Ubest-50 spectrophotometer. Fluorescence lifetime measurements were performed with a Horiba NAES 1100 time-resolved spectrofluorometer which uses a time-correlated single photon counting technique. Transient absorption spectra were observed with a nanosecond diffuse reflectance laser photolysis system, the setup of which was similar to that described previously.[17,18]

3. Results and Discussion

3.1. Steady-state Fluorescence Study on the An−MV^{2+} and APTAB−MV^{2+} Pairs. We observed fluorescence spectra of An in the absence and presence of MV^{2+} (data not shown). Quenching of the An fluorescence by MV^{2+} was not greatly affected by the existence of PS latex particles in the samples that were prepared by the procedure described in the Experimental Section. This D−A pair gives Stern−Volmer plots similar in shape for an aqueous solution and a PS latex dispersion. After repeated experiments, it turned out that the adsorption of An onto the latex particles was not equilibrated in the samples, and that more than 5 days were needed for the adsorption of An to be equilibrated. In addition, more than 99% of An molecules were adsorbed onto the latex particles in the equilibrated samples. The fluorescence quenching in the equilibrated latex samples was significantly suppressed compared with that in aqueous homogeneous solutions. This seems to be because An molecules deeply penetrate into the latex particles due to their hydrophobicity and very low solubility in water.

In contrast to An, APTAB fluorescence is markedly quenched by MV^{2+} on going from an aqueous homogeneous solution to a PS latex dispersion (Figure 2). Figure 2 demonstrates that the quenching in the latex dispersion is effectively brought about even when MV^{2+} concentration is lowered to 1 μM, which is two thousand times smaller than the concentration needed for the quenching in aqueous solutions. This means that PET in the latex dispersions takes place about two thousand times more efficiently than PET in aqueous solutions. The marked enhancement of PET can be ascribed to the increase in local concentrations of the donor and acceptor on the latex surface, as confirmed by the measurements of the adsorption isotherms (data shown later). The MV^{2+} used is a dichloride, and the pH value of the aqueous solution is about 6.6 across the concentration range in Figure 2b. At this pH, both APTAB and MV^{2+} exist in cationic forms. Thus, electrostatic attractions between these cationic probes and negative sulfate groups on the latex surface seem to play a major role in their adsorption.

In Figure 3, we show plots of the APTAB fluorescence intensity ratio against MV^{2+} concentration in an aqueous homogeneous solution and a PS latex dispersion. In the homogeneous aqueous solution, we added 2000 μM NaCl, because the fluorescence of APTAB was not quenched but enhanced by a small amount (5 μM) of MV^{2+} in the absence of NaCl. The reason for this peculiar behavior of the fluorescence of APTAB is currently unclear. One plausible reason is that APTAB molecules undergo self-quenching resulting from

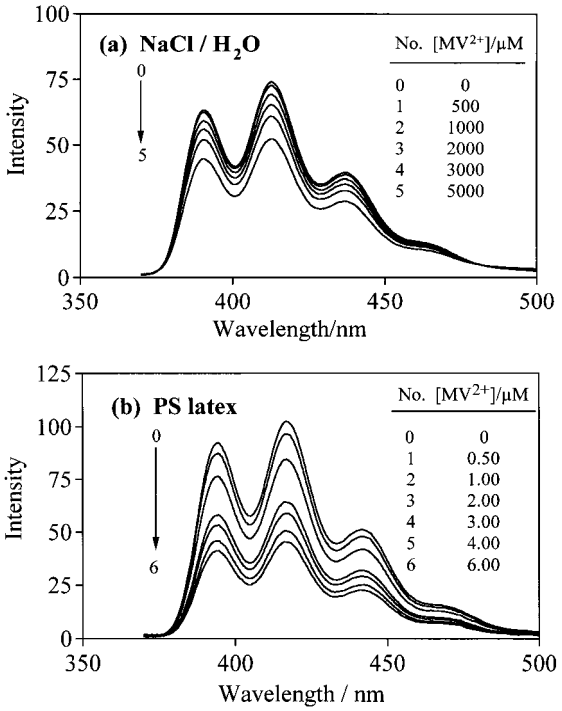

Figure 2. Fluorescence spectra of APTAB in the absence and presence of MV^{2+}. (a) Aqueous solution: [APTAB] = 1.0 μM; the samples are excited at 350 nm; excitation and emission band passes are 1.5 and 10 nm, respectively. (b) PS latex dispersion: [APTAB] = 1.0 μM; [PS] = 1.00 g/L; the samples are excited at 350 nm; excitation and emission band passes are 3 and 5 nm, respectively. The spectra for PS latex dispersion are corrected for the background scattering of excitation light.

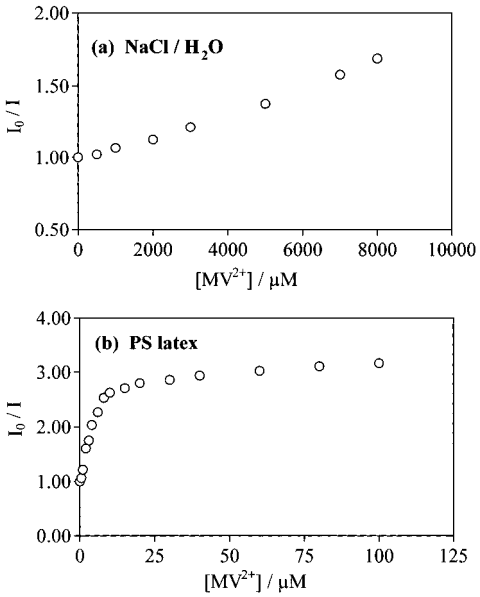

Figure 3. Stern−Volmer plots for the systems in Figure 2: (a) NaCl aqueous solution; (b) PS latex dispersion. Several data are added to those in Figure 2.

a formation of dimers or higher order aggregates, because this compound has an amphiphilic structure (see Figure 1). However, the addition of salts into aqueous solutions of amphiphiles generally enhances formation of aggregates and micelles. Therefore, formation of the aggregates does not seem to be the case for the present system. Because a butyltrimethylammonium derivative of pyrene also showed a similar behavior, we will investigate this problem in a future work. The plot for the aqueous solution is roughly linear (slightly upward curving),

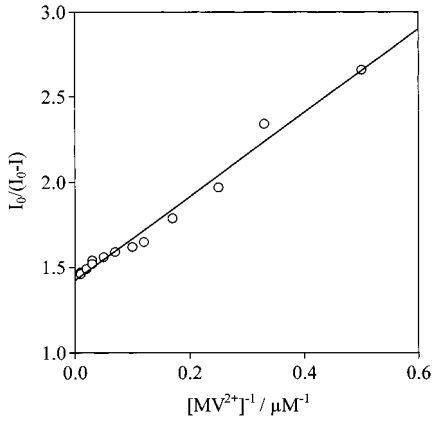

Figure 4. Modified Stern−Volmer plot for the systems in Figure 3b.

giving Stern−Volmer constant of 80 M^{-1}. The upward curving nature of the Stern−Volmer plot might be caused by a complex formation between APTAB and MV^{2+} because An and MV^{2+} form a charge-transfer complex.[19]

In contrast to the plot for the aqueous solution, that for the latex dispersion shows a downward curve. Such downward-curving plots were investigated by Eftink and Ghiron[20,21] for various cases. According to them, a downward-curving plot is obtained when a fluorophore is distributed in two or more different environments which have different accessibility to fluorescence quenching (*heterogeneously emitting system*). In our latex systems, it is difficult to analyze the downward curve (Figure 3b) in terms of the general treatment by Eftink and Ghiron, because their treatment contains too many parameters to be determined. Therefore, we used the simpler treatment proposed by Lehrer.[22] If we denote two environments as a (accessible to quenching) and b (inaccessible), a quantitative expression for the relation between fluorescence intensity and quencher concentration ([*Q*]) is given by the following equation.

$$I_0/(I_0 - I) = 1/f_a K_a[Q] + 1/f_a \quad (1)$$

$$f_a = I_{0a}/(I_{0a} + I_{0b}) = I_{0a}/I_0 \quad (2)$$

Equation 1 shows a linear relation between $1/[Q]$ and $I_0/(I_0 - I)$. We plot $I_0/(I_0 - I)$ against $1/[MV^{2+}]$ in Figure 4, where the total concentration of MV^{2+} in the latex dispersion is used instead of the local concentration on the latex surface, because the quencher is probably distributed two-dimensionally on the latex surface. The plot in Figure 4 shows a linearity to some extent between $I_0/(I_0 - I)$ and $1/[MV^{2+}]$, although the treatment is too simplified. From the intercept and the slope, we obtained $f_a = 0.70$ and $K_a = 5.71 \times 10^5$ M^{-1}. This Stern−Volmer constant is apparent and does not have its original meaning, because the quencher concentration is expressed by a total concentration in the dispersion despite the fact that the quenching mostly takes place on the latex surface. Thus, the extraordinarily large value of K_a reflects the increase in the local concentration of the quencher on the latex surface. However, if we consider the K_a value as a measure of concentrating effect of the latex surface on the reactants, we can realize that the PET reaction is remarkably enhanced on going from an aqueous solution ($K_a = 80$ M^{-1}) to the latex dispersion ($K_a = 5.71 \times 10^5$ M^{-1}).

It is necessary for us to get insights into environments a and b for substantiating the above-mentioned analysis. The accessible environment a is probably the surface of the latex particles, which is exposed to water. As for the inaccessible site b, there

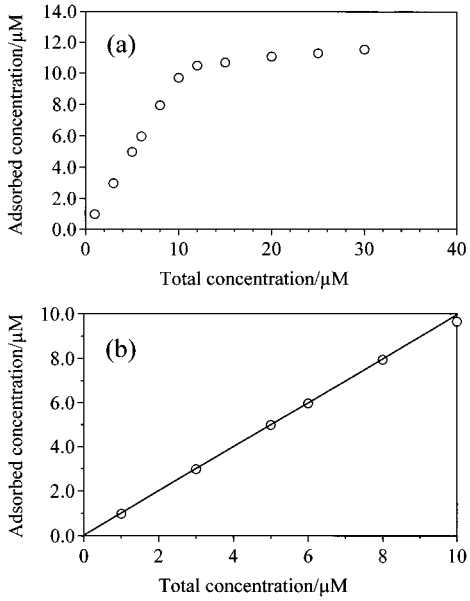

Figure 5. Adsorption isotherms of APTAB onto PS latex particles at 20 °C: (a) high concentration range and (b) low concentration range. [PS] = 1.00 g/L. The horizontal axis represents the total concentration of APTAB in the latex dispersion, and vertical axis represents the concentration of adsorbed APTAB. Accordingly, the slope of the line gives the mole fraction of APTAB adsorbed on the latex particles.

seem to be three candidates: (i) some kind of hole inside the latex particles, in which APTAB can diffuse but MV^{2+} cannot; (ii) some APTAB-adsorbed sites that are completely surrounded by other APTAB molecules, so that MV^{2+} molecules cannot approach those sites; (iii) an aqueous phase in which the quenching of APTAB fluorescence by MV^{2+} is inefficient at low concentrations such as several tens of micromolar. First, we consider case iii. In this case, the fraction of APTAB population on the latex surface should be close to f_a (= 0.70), assuming that the quantum yield of APTAB does not change much on going from aqueous phase to the latex surface (see eq 2). To obtain the fraction of APTAB on the latex surface, we observed the adsorption isotherm (Figure 5). The horizontal axis of Figure 5 represents the total concentration of APTAB in the latex dispersion, and the vertical axis represents the concentration of adsorbed APTAB, which is calculated as the difference between the total concentration in the dispersion and the equilibrium concentration in the supernatant. Accordingly, the slope of the line in Figure 5b gives the mole fraction of APTAB on the latex particles. It is elucidated from Figure 5b that 99% of APTAB exists on the latex particles when the concentration of APTAB is less than 10 μM. This value (0.99) is much greater than the value of f_a (0.70) obtained from Figure 4. Therefore, we rule out case iii. Next, we consider case i; we consider that a portion of APTAB molecules on the latex particles is accommodated in some hole, in which APTAB can diffuse but MV^{2+} cannot. In this situation, APTAB molecules in the hole are not susceptible to quenching. As MV^{2+} is a dication under the experimental condition, it is likely that there are hydrophobic holes inside the latex particles, in which the An chromophore of APTAB can diffuse but MV^{2+} cannot because of its highly ionic nature. In case ii, the adsorbed APTAB on the PS latex surface is sited irregularly. Some of the adsorbed APTAB are completely surrounded by other APTAB. Thus the adsorbed MV^{2+} is far away from the APTAB on the latex surface, and therefore cannot quench the fluorescence of the APTAB. This factor will become more significant when the occupation ratio (occupied sites/total sites) of APTAB is higher on the PS latex

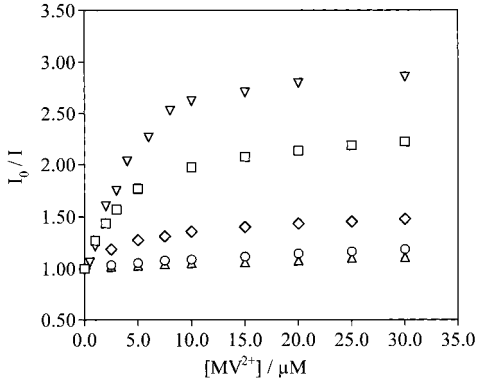

Figure 6. Stern−Volmer plots for the fluorescence of APTAB at different occupation ratios in the PS latex dispersions at 20 °C. Occupation ratios: ∇, 0.08; □, 0.42; ◇, 0.67; ○, 0.83; Δ 1.0.

surface. Figure 6 shows clearly that the quenching efficiency decreased greatly with the increasing of APTAB occupation ratio. This result can be understood easily because the adsorbed ATPAB cannot be replaced easily by MV^{2+}, but the adsorbed MV^{2+} can be replaced easily by APTAB in the PS latex dispersions. In conclusion, both cases i and ii seem to explain the present inaccessible site b. The difference between the two values (0.70 and 0.99) cannot be attributed to the breakdown of the assumption that the quantum yield of APTAB is not greatly affected by the latex surface. The quantum yield of APTAB actually is affected by the latex surface. However, the quantum yield is increased on going from aqueous phase to the latex surface, which will lead to a larger f_a value than the mole fraction on the latex surface. This tendency is opposite to the observed result.

Here we discuss the adsorption isotherm of APTAB in more detail. When the total concentration of APTAB is less than 10 μM in the experimental condition, the adsorption isotherm is a straight line with a slope of 0.99. This means that 99% of APTAB are adsorbed onto the PS particle surfaces. We found that cationic aromatic species adsorb onto the sites of anionic sulfate groups on PS latex particles.[23] After the anionic sites are completely occupied, a plateau or plateaulike part will appear in the adsorption isotherm. This can also be seen clearly in Figure 5a. The adsorption isotherm of MV^{2+} onto the PS particles has the same shape (data not shown). This kind of downward adsorption isotherm indicates that the adsorption coefficient of MV^{2+} decreases with increasing total concentration, so that the local concentration of MV^{2+} on the latex surface does not increase linearly with the total concentration. Furthermore, the profile of the Stern−Volmer plot is similar to that of the adsorption isotherm. Therefore, the downward-curving nature in Stern−Volmer plot for the latex systems (Figure 3b) seems to be ascribed, in part, to the adsorption behavior of MV^{2+}.

3.2. Time-resolved Fluorescence Study on the APTAB−MV^{2+} Pair. To obtain an insight into the mechanism of quenching of APTAB fluorescence by MV^{2+}, we observed the fluorescence decay curves (Figure 7). As seen in Figure 7, the fluorescence lifetime of APTAB is significantly decreased when MV^{2+} is coexistent. It turned out that the decay curves of APTAB in the latex dispersion are conformed to a double-exponential function even when MV^{2+} is absent:

$$I(t) = A_1 \exp(-t/\tau_1) + A_2 \exp(-t/\tau_2) \qquad (3)$$

where τ_1 and τ_2 denote the lifetime of each component, and A_1 and A_2 are preexponential factors. We obtained, from Figure

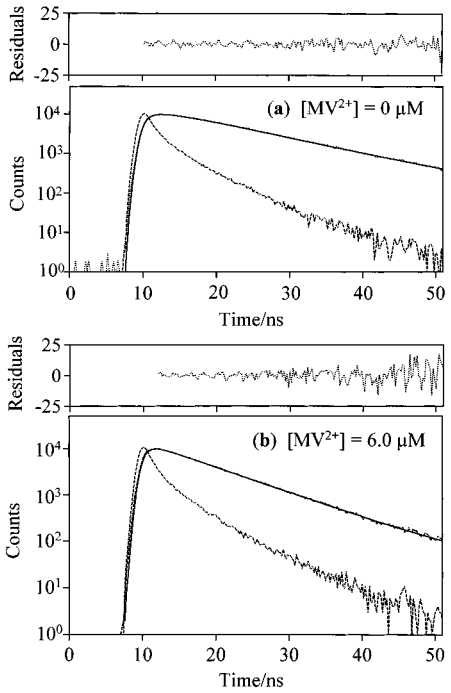

Figure 7. Fluorescence decay curves of APTAB in PS latex dispersions: (a) in the absence of MV^{2+}, and (b) in the presence of MV^{2+} (6.0 μM). [APTAB] = 1.00 μM; [PS] = 1.00 g/L. The samples are excited at 350 nm, and the excitation band pass is 14 nm. The emission is collected through a Toshiba L39 cutoff filter. A band-pass filter (U340) was put between the excitation monochromator and the sample to reduce a stray light, which is the main cause of background scattering from the latex samples.

7a ([MV^{2+}] = 0 μM), τ_1 = 4.1 ns (A_1 = 0.040) and τ_2 = 11.2 ns (A_2 = 0.068). The decay curve seems to have a two-component nature because APTAB is partitioned in two different milieus on the PS latex particles.

An analysis of the decay component is useful for obtaining information about whether the quenching is *dynamic* or *static*.[12,13] In dynamic quenching, τ_i (i = 1 or 2), is decreased with increasing quencher concentration, whereas A_i is not changed. In static quenching, on the contrary, A_i is decreased with increasing quencher concentration, whereas τ_i remains constant. We tried to examine the dependence of each of the decay components on MV^{2+} concentration. However, the instrument response function is not short enough to allow it. Thus, we used the average lifetime.[13]

$$\langle\tau\rangle = \Sigma A_i\tau_i^2/\Sigma A_i\tau_i \qquad (4)$$

We plot $\langle\tau\rangle_0/\langle\tau\rangle$ against MV^{2+} concentration in Figure 8. The Stern−Volmer plot for the average lifetime is also downward curving as is the plot for steady-state fluorescence intensity (Figure 3b). However, if we carefully compare Figure 8 with Figure 3b, we notice the difference between them. The I_0/I value reaches 2.8 at [MV^{2+}] = 20 μM, whereas $\langle\tau\rangle_0/\langle\tau\rangle$ is 1.7 at the same MV^{2+} concentration. The difference can be attributed to a contribution from the fraction which is operated by static quenching mechanism. Therefore, we conclude that the PET quenching on the latex surface is operated by both static and dynamic mechanisms.

3.3. Steady-state Fluorescence and Diffuse Reflectance Laser Flash Photolysis Studies on the Py−MV^{2+} pair. In general, there are two purposes for using solid surfaces as substrates for PET: (1) to enhance PET by condensing and orienting the reactants, and (2) to suppress the back electron

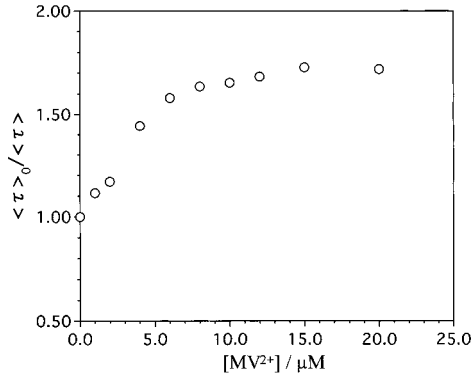

Figure 8. The Stern−Volmer plot for the average lifetime of APTAB fluorescence in PS latex dispersions. [APTAB] = 1.00 μM; [PS] = 1.00 g/L.

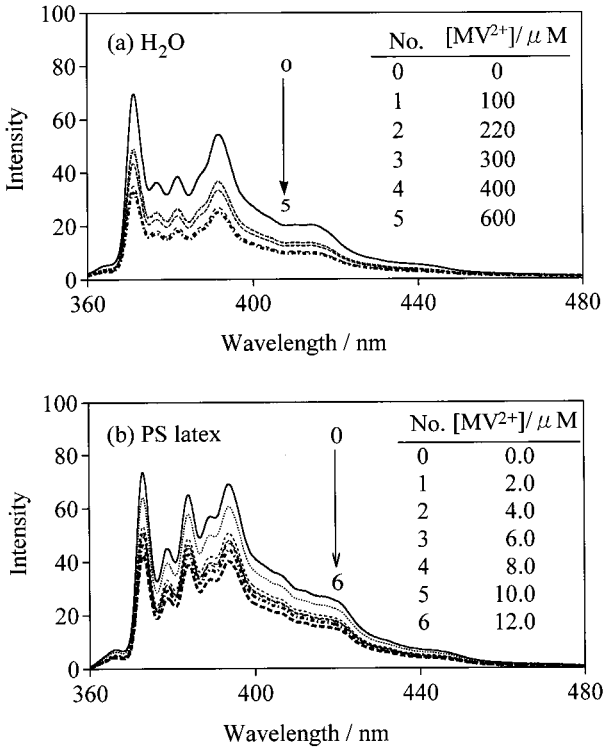

Figure 9. Fluorescence spectra of Py in the absence and presence of MV^{2+}. [Py] = 0.51 μM; [PS] = 1.00 g/L.

transfer to achieve effective charge separation.[24] We have shown in Figure 2 the usefulness of the PS latex particles for realizing purpose (1). To examine purpose 2, we intended to observe transient absorption spectra. Because the latex dispersion is turbid like a milk, a conventional (i.e., transmittance mode) flash photolysis technique is of no use for the system. Therefore, we used the diffuse reflectance mode. First, we used APTAB/PS dispersion to measure the transient absorption spectrum, but the signal was very weak. This may have been caused by decomposition of the probe molecules, the small size of the extinction coefficient of the An cation radical, and/or the fastness of the back electron transfer. We then examined Py/MV^{2+}/PS dispersion to reach this goal.

Before we performed flash photolysis experiments, we confirmed by steady-state fluorescence spectroscopy that the PET from Py to MV^{2+} is remarkably enhanced on going from the aqueous homogeneous solution to the latex dispersion (Figure 9). As seen from Figure 9, the fluorescence of Py is effectively quenched by MV^{2+} in the latex dispersion even when MV^{2+} concentration is at a micromolar level, which is several

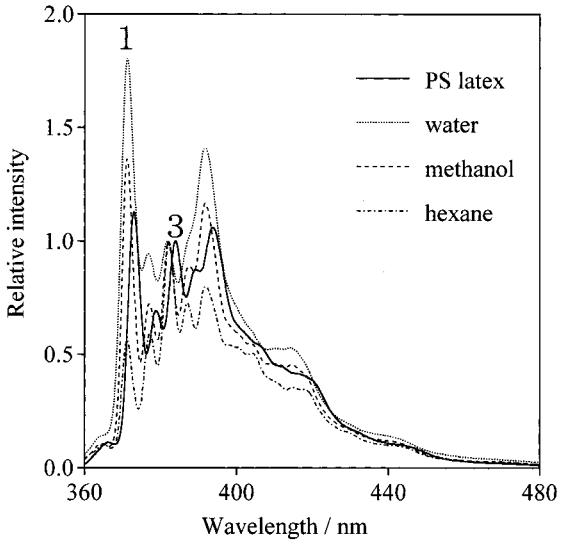

Figure 10. Fluorescence spectra of Py in a PS latex dispersion and in homogeneous solutions.

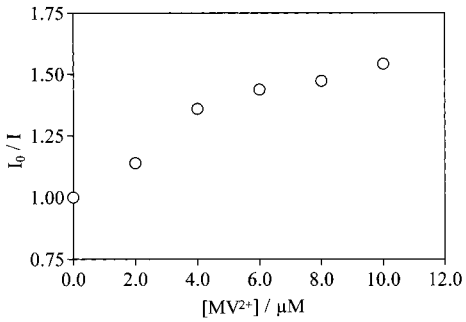

Figure 11. The Stern−Volmer plot for the systems in Figure 9b.

tens of times smaller than that needed for the quenching in aqueous solutions. This means that PET in the latex dispersions takes place several tens of times more efficiently than that in aqueous solutions. The marked enhancement of PET can be ascribed to the increase in local concentrations of the donor and acceptor on the latex surface, as confirmed by the adsorption isotherms (data not shown). The effective adsorption of the donor (Py) onto the latex surface is also evidenced by the vibronic fine structure of the fluorescence. The intensity ratio between bands 1 and 3 (so-called I_1/I_3 value; see Figure 10) is well-known to be a measure of polarity around the probe.[25,26] The I_1/I_3 value obtained is 1.13 for the latex dispersion, which is much closer to the values for benzene (1.05)[26] and 1-propanol (1.09)[26] than the value for water (1.81). This means that most Py molecules are located on the latex particles.

In Figure 11, we show the Stern−Volmer plot for the Py/MV^{2+}/PS dispersion. The Stern−Volmer plot is downward curving as in APTAB. Although we also made the modified Stern−Volmer plot, the linearity between $I_0/(I_0 - I)$ and $1/[MV^{2+}]$ is too poor to be used for further analysis (data not shown). This poor linearity might be caused by the simplicity of the two-site quenching model by Lehrer. However, we can roughly estimate the fraction of Py molecules at the accessible site from Figure 11. The value of I_0/I reaches a plateau value of about 1.5 (= 3/2) in the higher concentration region of MV^{2+}. Because I_0/I is equal to $(I_{0a} + I_{0b})/I_{0b}$ after the fraction at the site *a* is completely quenched, we obtain $(I_{0a} + I_{0b})/I_{0b} = 3/2$. This means that about 33% of Py molecules are located at the accessible site. The fraction of Py at site a is much smaller than that for APTAB ($f_a = 0.70$). Because Py is more hydrophobic

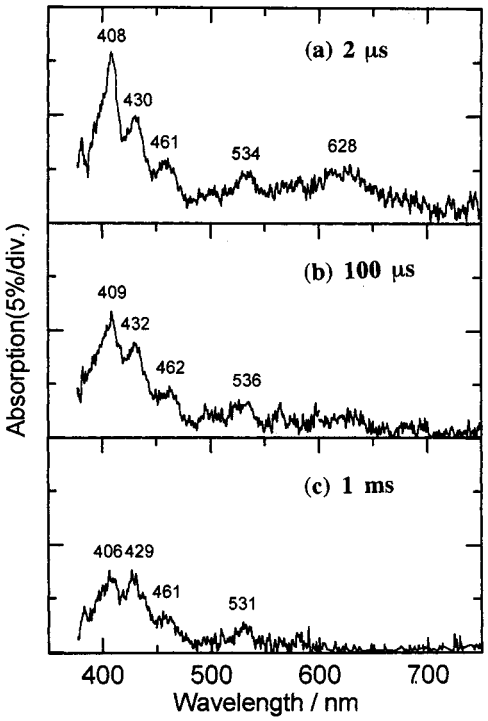

Figure 12. Transient absorption spectra of Py−MV^{2+} pair in a PS latex dispersion. Concentrations: [Py] = 250 μM, $[MV^{2+}]$ = 300 μM; [PS] = 54.2 g/L .

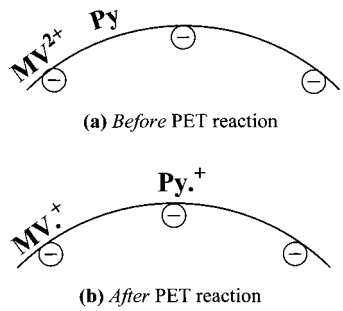

Figure 13. Schematic representation for the behavior of Py, MV^{2+}, and their PET reaction products on a PS latex surface.

than APTAB, considerable portion of Py molecules might be buried inside PS latex particles, resulting in protection from quenching by MV^{2+}.

The transient absorption spectra for the PS latex dispersion containing Py and MV^{2+} are shown in Figure 12. The band at 408 nm is assigned to the $MV^{\bullet+}$ cation radical, and the band at 461 nm is assigned to the $Py^{\bullet+}$ cation radical.[27] According to Figure 12, these radical bands remain for more than 1 ms. If we consider that charge recombination between the PET products usually occurs in a much shorter time in homogeneous solutions, we realize that the back electron transfer is markedly suppressed in the latex dispersion. Thus, the present result demonstrates the usefulness of the latex system for performing effective charge separation.

To understand the remarkable effect of the latex system on suppression of charge recombination, we present in Figure 13 a schematic picture for the behaviors of the reactants and products of the PET reaction on the latex surface. Before the PET reaction, Py molecules are mostly adsorbed onto the continuous PS area by hydrophobic interaction, whereas MV^{2+} molecules are anchored at the sulfate groups by electrostatic attraction. After the PET reaction, both of the products will be fixed at the sulfate groups because of electrostatic interaction.

The fixation of the products seems to result in suppression of the back electron transfer.

Recently, Hsiao and Webber[28,29] investigated PET reactions from Py and An derivatives to a viologen analogue using a PS latex dispersion. They also observed a remarkable increase in the efficiency of charge separation for some donor−acceptor pairs, although the forward PET reactions were not improved by the use of the latex dispersion. They ascribed the remarkable increase in the yield of the charge separation to the "compartmentalization effect" of the latex particles. It is likely that there are compartments (holes) on the latex surface which accommodate limited kinds of the products and/or reactants. The existence of the compartments is also suggested in our experiments for the present and another system.[5] In conclusion, it seems that both "fixation effect" and "compartmentalization effect" play an important role in PET processes in the latex systems.

4. Conclusions

We have shown from steady-state fluorescence measurements that PET from APTAB to MV^{2+} is about two thousand times enhanced on going from the aqueous homogeneous solution to the PS latex dispersion. This is attributed to the increase in local concentrations of both APTAB and MV^{2+} on the latex surface, as evidenced by their adsorption isotherms. The Stern−Volmer plot for APTAB−MV^{2+} in the aqueous homogeneous solution is almost linear, with a quenching constant of 80 M^{-1}, while the plot for the same pair in the latex dispersion becomes downward-curving. The downward curve is explained, in part, by a model of a *heterogeneously emitting system*,[20−22] which assumes the distribution of a fluorophore in two environments: one is accessible to quenching and the other is not. The change of the adsorption coefficient of MV^{2+} onto the latex particles is also responsible for the deviation of the Stern−Volmer plot from linearity. In contrast to APTAB−MV^{2+}, quenching of the An fluorescence by MV^{2+} was suppressed by the existence of PS latex particles. This may be because the An molecule is buried deeply inside the latex particles due to its hydrophobicity and low solubility in water.

The mechanism of PET quenching of the APTAB−MV^{2+} pair in the latex dispersion has been examined by time-resolved fluorescence measurements. The fluorescence decay curves of APTAB show a double-exponential nature in the latex dispersion, reflecting the distribution of this fluorophore between two different milieus on the latex particles. The dependence of the fluoresence lifetime of APTAB on MV^{2+} concentration demonstrates that the PET quenching on the latex surface is operated by both static and dynamic mechanisms.[12,13]

PS latex surfaces not only improve the forward electron transfer significantly, but also suppress back electron transfer effectively. The suppression of the back electron transfer is confirmed by observation of the transient absorption of $MV^{\bullet+}$ and $Py^{\bullet+}$ cation radicals by use of diffuse reflectance laser flash photolysis technique. These results demonstrate the usefulness of the latex system for performing effective charge separation.

Acknowledgment. The authors thank Professor Fumio Kato (Saga University) for the use of their Hitachi 55p-72 ultracentrifuge. The cost of this work is partly defrayed by the Grant-in-Aid for Scientific Research on Priority-Area-Research "Photoreaction Dynamics" from the Ministry of Education, Science, Sports, and Culture of Japan (No. 08218249).

References and Notes

(1) Nakashima, K.; Duhamel, J.; Winnik, M. A. *J. Phys. Chem.* **1993**, *97*, 10702.
(2) Nakashima, K.; Liu, Y. S.; Zhang, P.; Duhamel, J.; Feng, J.; Winnik, M. A. *Langmuir* **1993**, *9*, 2825.
(3) Nakashima, K.; Kido, N. *Photochem. Photobiol.* **1996**, *64*, 296.
(4) Nakashima, K.; Miyamoto, T.; Hashimoto, S. *Chem. Commun*. **1999**, 213.
(5) Nakashima, K.; Tanida, S.; Miyamoto, T.; Hashimoto, S. *J. Photochem. Photobiol. A: Chem.* **1998**, *117*, 111.
(6) Nakashima, K.; Kido, N.; Yekta, A.; Winnik, M. A. *J. Photochem. Photobiol. A: Chem.* **1997**, *110*, 207.
(7) Stramel, R. D.; Nguyen, C.; Webber, S. E.; Rodgers, M. A. J. *J. Phys. Chem.* **1988**, *92*, 2934.
(8) Martens, F. M.; Verhoeven, J. W. *J. Phys. Chem.* **1981**, *85*, 1773.
(9) Fornasiero, D.; Grieser, F. *J. Chem. Soc., Faraday Trans.* **1990**, *86*, 2955.
(10) Hsiao, J.-S.; Webber, S. E. *J. Phys. Chem.* **1992**, *96*, 2892.
(11) Gehlen, M. H.; DeSchryver, F. C. *J. Phys. Chem.* **1993**, *97*, 11242.
(12) Birks, J. B. *Photophysics of Aromatic Molecules*; Wiley-Interscience: London, 1970.
(13) Lakowicz, J. R. *Principles of Fluorescence Spectroscopy;* Plenum: New York, 1986.
(14) Charreyre, M.-T.; Zhang, P.; Winnik, M. A.; Pichot, C.; Graillat, C. *J. Colloid Interface Sci.* **1995**, *170*, 374.
(15) Davis, W. W.; Krahl, M. E.; Clowes, G. H. A. *J. Am. Chem. Soc*. **1942**, *64*, 108.
(16) Dabestani, R.; Ivanov, I. N. *Photochem. Photobiol*. **1999**, *70*, 10.
(17) Hashimoto, S.; Fukazawa, N.; Fukumura, H.; Masuhara, H. *Chem. Phys. Lett*. **1994**, *223*, 493.
(18) Hashimoto, S. *Chem. Phys. Lett*. **1996**, *252*, 236.
(19) Dabestani, R.; Reszka, K. J.; Sigman, M. E. *J. Photochem. Photobiol. A: Chem.* **1998**, *117*, 223.
(20) Eftink, M. R.; Ghiron, C. A. *Biochemistry* **1976**, *15*, 672.
(21) Eftink, M. R.; Ghiron, C. A. *Anal. Biochem*. **1981**, *114*, 199.
(22) Lehrer, S. S. *Biochemistry* **1971**, *10*, 3254.
(23) A similar example is the adsorption of cationic surfactant on PS latex particles: Connor, P.; Ottewill, R. H. *J. Colloid Interface Sci.* **1971**, *37*, 642.
(24) Kalyanasundaram, K. *Photochemistry in Microheterogeneous Systems*; Academic Press Inc.: New York, 1987.
(25) Kalyanasundaram, K.; Thomas, J. K. *J. Am. Chem. Soc*. **1977**, *99*, 2039.
(26) Dong, D. C.; Winnik, M. A. *Photochem. Photobiol.* **1982**, *35*, 17.
(27) Slama-Schwok, A.; Ottolenghi, M.; Avnir, D. *Nature* **1992**, *355*, 240.
(28) Hsiao, J.-S.; Webber, S. E. *J. Phys. Chem.* **1993**, *97*, 8289.
(29) Hsiao, J.-S.; Webber, S. E. *J. Phys. Chem.* **1993**, *97*, 8296.